Hair Cell Generator Potentials

DANIEL L. ALKON and ANTHONY BAK

From the Laboratory of Neurophysiology, National Institute of Neurological Diseases and Stroke, National Institutes of Health, Bethesda, Maryland 20014

ABSTRACT A technique is introduced using a piezoelectric device to stimulate hair cells of a molluscan statocyst while recording their responses intracellularly. Statocyst displacements produced with the technique are calibrated with stroboscopic photography. Properties of the hair cells' response to currents and mechanical stimulation are studied. The hair cell generator potential arises from a conductance increase and, for a certain range, is a logarithmic function of the amplitude of the displacement stimulus.

Gastropod molluscan statocysts (Wolff, 1969; Coggeshall, 1969) consist of ciliated cells ("hair cells"[1]) which form a hemisphere containing concretions (statoconia or statoliths) floating within the fluid (statolymph) of the cyst. Extracellular recordings (Wolff, 1968, 1970 *a*, *b*) from pulmonate hair cells' axons in the static nerve demonstrated that the statocyst responds to position changes with specific signals which precede a stereotypic behavioral reflex. The animal reflexly returns to the position of minimal hair cell activity (i.e. the head-up position) irrespective of the direction in which it is moved from that position.

Hair cells are found in the inner ear and lateral line organs of fish and amphibians as well as in the vestibular labyrinth of mammals. Electrical responses of lateral line organs have been shown (recording extracellularly) to be proportional to displacement of these organs (Jielot et al., 1952; Kuiper, 1956; Flock, 1965). Similar proportionality to displacement was seen in the slow responses recorded from the crista ampullaris in the semicircular canals (Trincker, 1957) and in the electrical output from the organ of Corti (von Bekesy, 1960). Harris et al. (1970) obtained intracellular recordings from hair cells in the tail lateral line of *Necturus maculosus* showing receptor potentials less than 800 μV peak to peak.

In this study intracellular recording is used to examine the nature of the hair cell's response to adequate stimulation as well as the relationship of that response to stimulus intensity and duration. Also examined are possible

[1] This term will be used although the cells studied here are not histologically identical to the "hair cells" described in vertebrates, i.e., cells with stereocilia, a kinocilium, and without axons.

mechanisms underlying the transduction of the mechanical stimulus into an electrical response.

METHODS

Preparation

Hermissenda were provided by Dr. Rimmon Fay of the Pacific Bio-Marine Supply Co. (Venice, Calif.).

The statocysts of *Hermissenda crassicornis* are located symmetrically under the integument at the junction of the pedal and cerebropleural ganglia. A transverse cut immediately beneath the anterior third of the animal causes the integument to retract exposing the circumesophageal ganglia, the two eyes, and the two statocysts. After all the connectives of the circumesophageal ganglia ring are cut (leaving the optic and statocyst nerves intact) the isolated nervous system is pinned in a chamber and immersed in synthetic seawater (Instant Ocean, Aquarium Systems, Inc., Eastlake, Ohio) at room temperature (22°C).

Intracellular Recording

A connective tissue sheath enveloping the isolated nervous system was partially digested with Pronase (Sigma Chemical Co., St. Louis, Mo.), a nonspecific protease, to facilitate insertion of the microelectrodes. A range of Pronase concentration (1.3 mg/cm^3 to 4 mg/cm^3) was found in which the statocyst was entirely intact while intracellular recordings were still possible. The spontaneous movements of the statoconia normally observable remained with this range of Pronase concentration. With excess Pronase, membrane resistance of hair cells decreased only slightly although the frequency of spontaneous firing increased significantly, and spontaneous movements of the statoconia ceased. Concentrations not exceeding 4 mg/cm^3 were, therefore, used in our experiments.

Intracellular recordings were made with glass micropipettes filled with 4 M potassium acetate and having a resistance of 60–80 MΩ. A Wheatstone bridge circuit was used for current passage through the recording electrode.

Stimulation of Hair Cells

Small displacements of the statocyst were produced by a piezoelectric crystal, barium titanate, deposited as a ceramic on a steel beam, $2\frac{1}{2}$ inches long, $\frac{1}{2}$ inch wide, and $^{17}/_{1000}$ inches thick (manufactured by Mullenbach Div., Cutler Hammer, Inc., Los Angeles, Calif.). When the beam is mechanically fixed at one end (here by a micromanipulator), and a voltage is applied across the device, the ceramic will deform, moving the free end of the beam. To this free end was attached a 30 gauge stainless steel needle. The pleural ganglion adjacent to the statocyst under study was fixed by suction to the blunt end of the needle.

Stroboscopic photography was used to calibrate the mechanical stimulus technique. 10-μs flashes were delivered to the preparation at specified delays after a voltage pulse to the piezoelectric device. Double flashes were also used to measure displacement (Fig. 1).

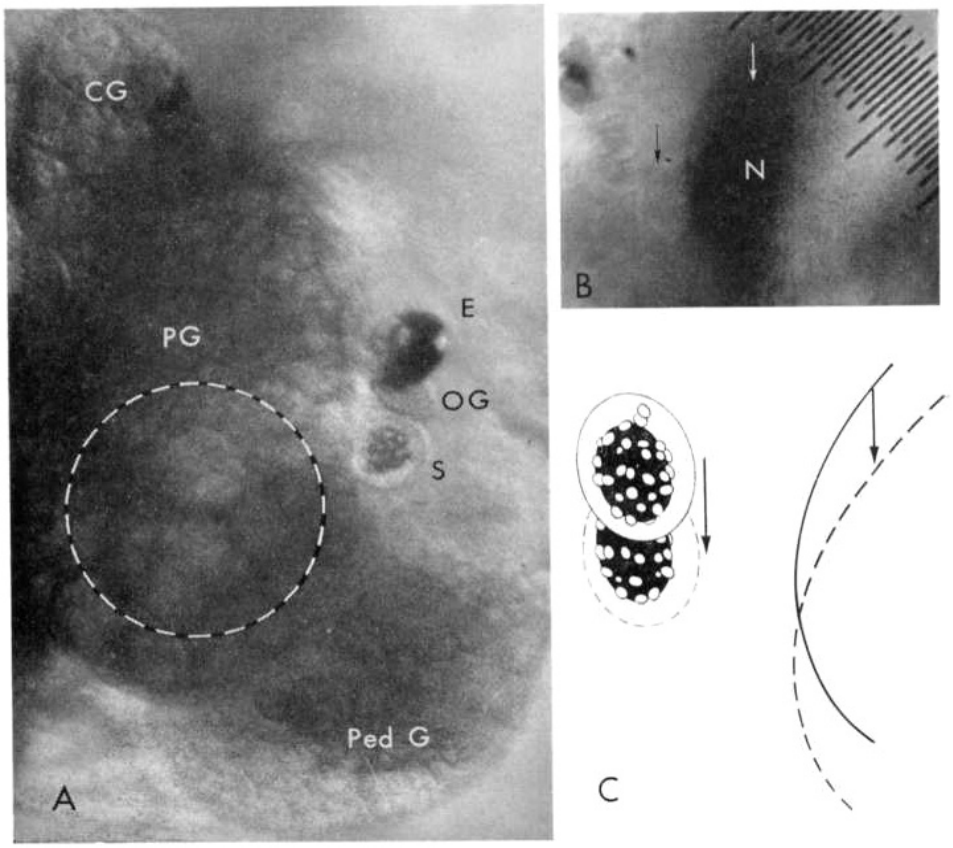

FIGURE 1. (A), Photograph of hemisection of circumesophageal nervous system of *Hermissenda* demonstrating the eye (E), optic ganglion (OG), statocyst (S), cerebral ganglion (CG), pleural ganglion (PG), and pedal ganglion (Ped G). The dashed circle indicates the position of the 30 gauge needle on the preparation. (B), Stroboscopic photograph of statocyst and pleural ganglion attached by suction to blunted 30 gauge steel needle. A 10 μs flash occurred first at 1.2 ms after the application of a 1.0 ms 90 V pulse to the piezoelectric device and then at 20 ms after the pulse. At 20 ms the cyst and beam are in their original positions to which they return within 2.0 ms of the pulse's initiation. Calibration: 2 small divisions = 25 μm (C), Tracing of this photograph enlarged 2.0$\times$ shows the cyst and beam in their original positions and 1.2 ms after the 90 V pulse.

RESULTS

Anatomy

A 3 μm section stained with toluidine blue (Fig. 2) demonstrates a *Hermissenda* statocyst. The cyst consists of a thin wall derived mainly from the hair cells themselves. A few concretions or statoconia are visible. Conventional histology showed the hair cells to be disk shaped, approximately 25–40

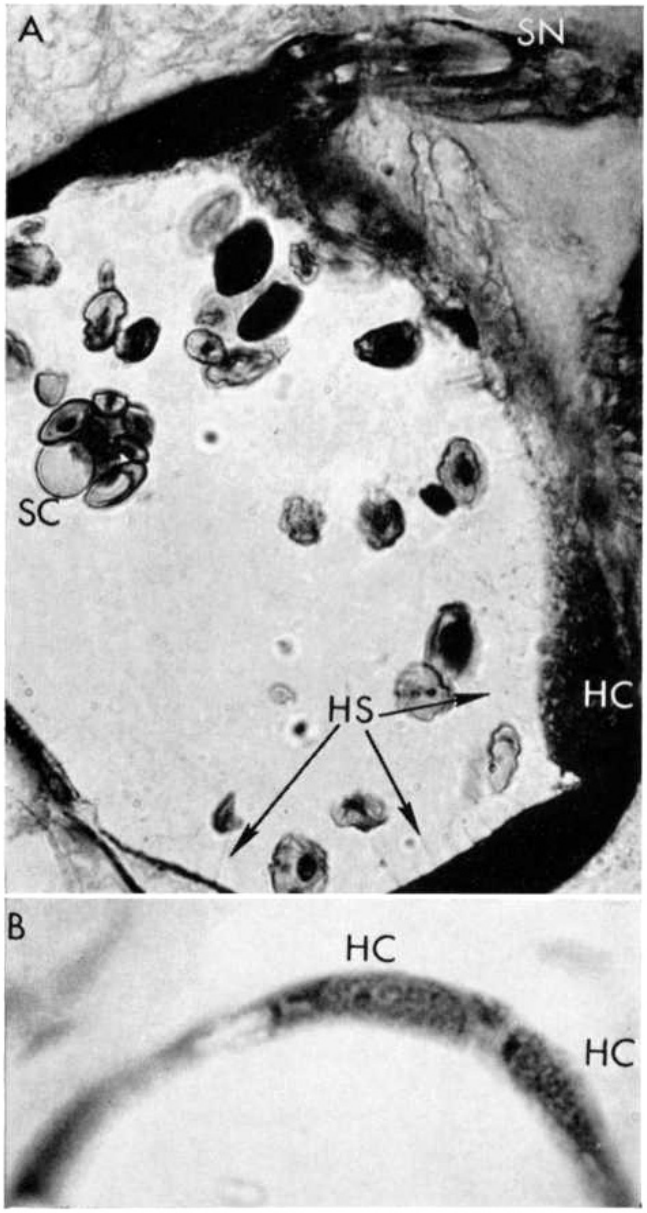

FIGURE 2. (A), A 3 μm section of *Hermissenda's* statocyst stained with toluidine blue. Statoconia (SC) are visible within the cyst. The hair cells (HC) comprise the wall of the cyst. Numerous small hairs (HS) project from the cell's surface. Hair cell axons enter the pleural ganglion via the static nerve (SN). × 1000. (B), A 3 μm section of *Hermissenda's* statocyst stained with toluidine blue. The figure shows two adjacent hair cells. The nuclei almost fill the cell bodies. × 1000.

μm in diameter, and 5–10 μm thick. Numerous hairs project from the cell's surface toward the cyst's center.

Stimulus Calibration

Recordings across the piezoelectric device (Fig. 3, inset) showed that a maximum voltage is reached in less than 150 μs for pulses of 20 V or less. A slower time constant applies for the later charging of the device with higher

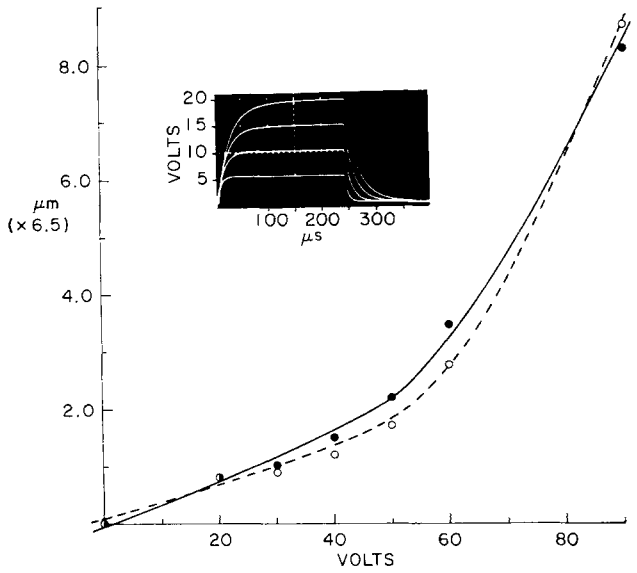

FIGURE. 3. Maximum displacement of beam (solid circles) and cyst (open circles) as a function of voltage as measured by stroboscopic photography. All pulses were of 1.0 ms duration. Measurements were obtained for the beam and statocyst simultaneously. Close mechanical coupling between the beam and statocyst is demonstrated. The final displacement varies linearly with voltage for pulses of less than 40 V. *Inset*, Voltage recordings directly across the piezoelectric device. A second slower time constant appears as voltage increases. Inputs: 5, 10, 15, 20 V.

voltage pulses. This was found to be a property of the voltage attenuator used and not the piezoelectric device itself.

Stroboscopic photography demonstrated that voltage intput to the crystal is directly proportional to the resulting displacement of the beam as well as to the displacement of the statocyst for inputs less than 40 V. Fig. 3 illustrates the rapid increase of displacement for higher voltages. The movement of the cyst closely follows that of the beam. This close mechanical coupling occurs in time as well. Fig. 4 compares the movement of the 30 gauge needle in air with that of the statocyst over 1.2 ms for a 1.0 ms 90 V pulse to the piezoelectric device. The rate of movement of the beam in air is almost

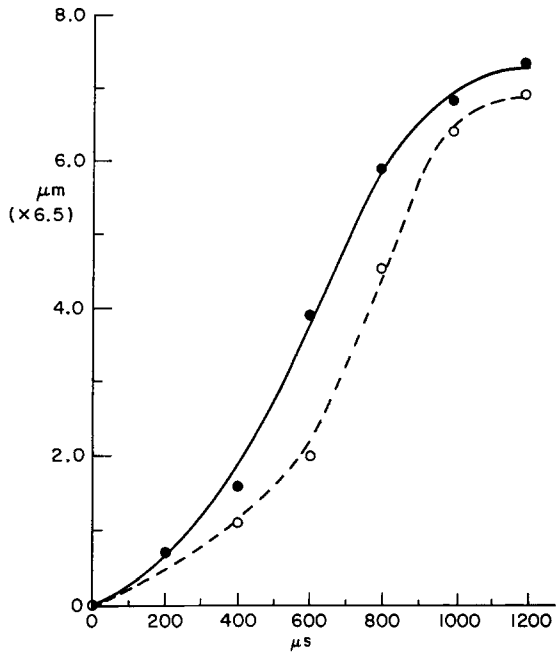

FIGURE 4. Displacement of beam (solid circles) and cyst (open circles) as a function of time measured by stroboscopic photography. A 90 V pulse of 1.0 ms duration was applied and 10-μs flashes were delivered at varying delays. The movement of the 30 gauge steel needle was measured when unattached to the preparation (average of two experiments). The statocyst (average of six experiments) closely follows the needle as it develops its maximum displacement over 1.2 ms.

identical to that of the cyst. Less time is required for the beam and cyst to reach maximal excursion for lower voltages. The statocyst reaches the excursion necessary for a maximum response (approximately 10 μm) in 0.5–0.6 ms and returns to its point of origin in the same time.

Comparison of the piezoelectric charging times (Fig. 3, inset) with the times necessary for movement of the beam and statocyst indicates that the mechanical event is more than 3 times slower than the electrical event. Small differences in charging times for different voltages applied to the device would, therefore, not be expected to significantly affect the velocity of displacement.

Stroboscopic photography was also used to measure the displacement of the statocyst with a microelectrode inserted into the cyst. The movement of the statocyst is in a plane approximately perpendicular to the axis of the electrode and that of the needle attached to the piezoelectric device. No appreciable difference in displacement was caused by the electrode. Nor was any distortion of the cyst by the electrode apparent. Presumably very little

resistance to movement was offered by the finely tapered end of the electrode which bends with the displacement of the statocyst.

Cell Penetration and Characteristics

Cell penetration was signaled by a sudden potential drop of 20–30 mV and an additional slower drop of 15–20 mV. DC hyperpolarizing current was often briefly applied to reduce injury discharge. Spikes, which invariably appeared with the first sudden potential shift signaling penetration, increased in size with the subsequent slower potential shift. Soon after penetration, the hyperpolarizing current now removed, the hair cells either did not fire spontaneously or fired with a frequency less than 200/min. In most cells frequent small depolarizing waves occurred. If the cell was depolarized only slightly above its resting level, spikes were frequently triggered by these spontaneous depolarizing waves. Base line activity, however, was complex including hyperpolarizing waves as well. This base line activity might arise either from the random spontaneous movements of the statoconia (observable under a dissecting microscope), from pacemaker activity of the hair cells themselves, and/or from synaptic input to the hair cells. Resting membrane potential as measured when withdrawing the electrode was approximately 45 mV and the time required for charging the membrane to $\left(1 - \frac{1}{e}\right) V_s$ (where V_s is the final value) was 19–26 ms in different cells. Semilogarithmic plots of the charging curves reveals, however, that charging time is controlled by more than one time constant.

Input resistance varied from 30 to 100 MΩ (Table I, Fig. 5A). Average spike size was 42 mV (Table I) and spike frequency varied linearly with current input (Fig. 6). Weak depolarizing currents often elicited small waves which may represent subliminal membrane responses (Fig. 6).

Mechanical Stimulation of Hair Cells

The onset of the displacement stimulus was signaled by an artifact associated with the voltage pulse applied to the piezoelectric device. The latency observable even with small displacements was less than 2 ms (Fig. 9 B). Displacement of the statocyst caused a depolarizing wave with superposed spikes in the hair cell. This depolarizing wave or generator potential increased in proportion to the voltage across the piezoelectric ceramic (and thus magnitude of displacement). Fig. 7 illustrates a typical intensity series and Fig. 8 shows linear and semilogarithmic plots of generator potential as a function of displacement magnitude. The frequency of superposed spikes (occurring during the first 60 ms of the response) varied directly with the

TABLE I
ELECTRICAL CHARACTERISTICS

	Time constants	Spike size	Resistance
	ms	*mV*	*MΩ*
	27.5	48	36.5
	23.1	32	44.0
	21.7	40	31.4
	22.6	50	51.5
	19.0	35	31.6
	23.0	32	25.5
	25.2	45	63.5
	19.5	35	35.7
	19.0	42	60.0
		43	55.5
		52	38.4
		31	35.7
		45	30.4
		50	70.2
		50	100.0
		45	35.1
		33	54.4
			109.0
			55.5
			86.7
			51.0
Average	22.3	42.1	52.5

magnitude of the generator potential when this potential exceeded spike threshold (Fig. 9 A).

Duration

When the voltage input was held constant and the duration of the stimulus varied, a maximal response was elicited with durations 0.5 to 1.0 ms (Fig. 10). The onset of the maximal response plateau is consistent with the time necessary (0.6 ms) to achieve maximal excursion of the piezoelectric beam for a 20–30 V input pulse (as measured by stroboscopic photography). If the duration was increased beyond 1.0 ms, the response of the hair cell decreased from its maximum. This decrease might be due to the presence of the electrode which because of its own stiffness might oppose the effect of displacement stimuli of durations greater than 1.0 ms. Increasing the duration of the voltage pulse across the piezoelectric crystal from 1.0 to 2.0 ms maintains the beam as well as the statocyst (as measured by stroboscopic photography) at the point of maximum excursion for a longer time. Thus, an oscillation of the cyst for these longer durations is unlikely although oscillation of the stataconia and/or sensory hairs is still possible.

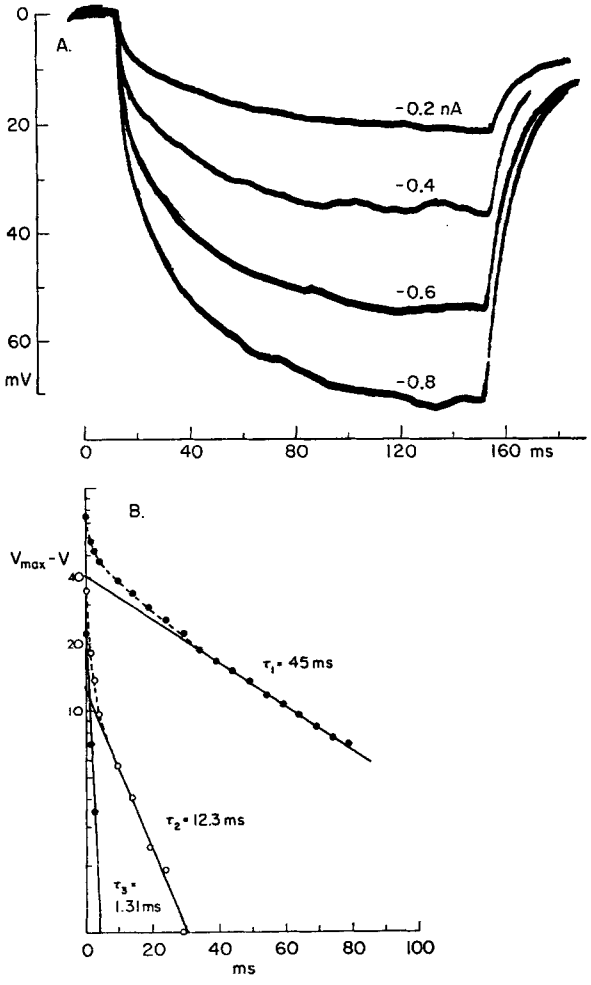

FIGURE 5

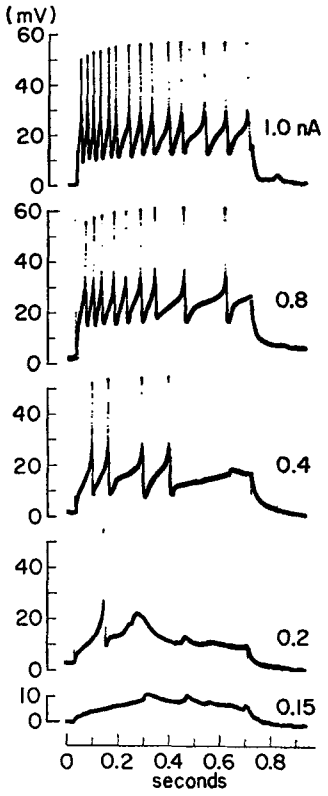

FIGURE 6

FIGURE 5. (A), Responses of hair cell to hyperpolarizing currents. Potential change varies linearly with current injected. (B), "Peeling" of time constants. For a given charging curve, voltage at varying times is subtracted from the maximum voltage achieved. The first time constant is obtained from the slope of the asymptote to the curve generated from a semilogarithmic plot of voltage difference vs. time. A second curve is generated by repeating the procedure subtracting points of the first plot from the asymptote. In this way, three time constants are obtained for the charging curve above, satisfying an equation of the form:

$$v(t) = Ae^{-\alpha t} + Be^{-\beta t} + Ce^{-\gamma t} + D,$$

where the time constants are the reciprocals of α, β, and γ. The charging of the electrode itself probably contributes the third (fast) time constant observed.

FIGURE 6. Responses of hair cell to depolarizing current. Small depolarizing waves occur much below threshold for weak currents. Spike frequency varies linearly with current input.

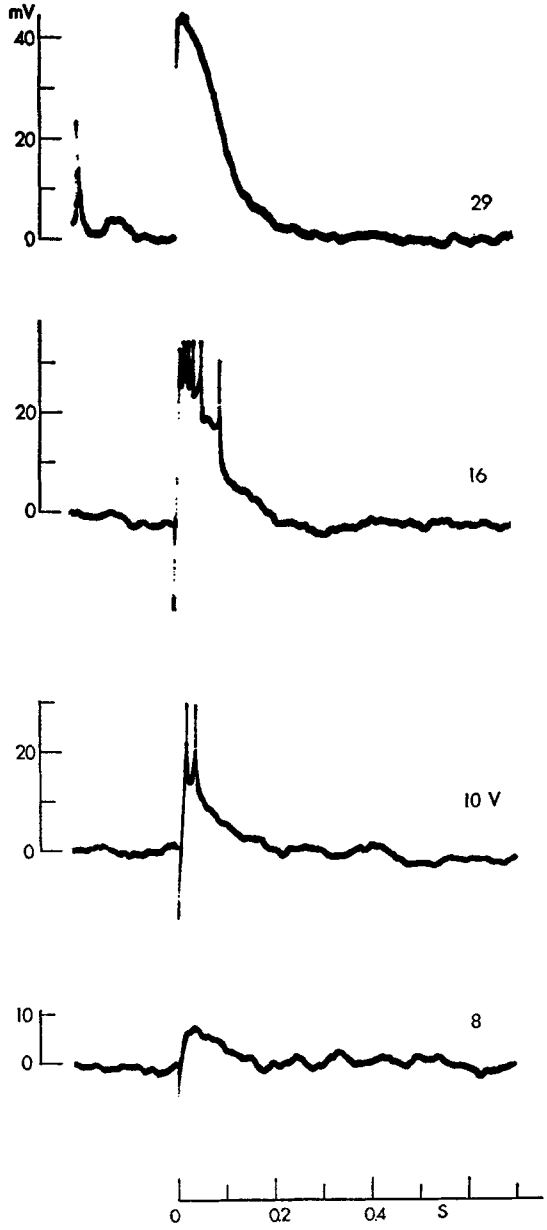

FIGURE 7. Hair cell responses to increasing displacement. Threshold stimulation at bottom of figure. Onset of stimulus is marked by down-going artifact at the beginning of the generator potential.

Adaptation

The responses in the intensity series discussed above were of necessity only transient. Steady-state responses could not be studied since static displacement of the statocyst usually causes the electrode to come out of the impaled

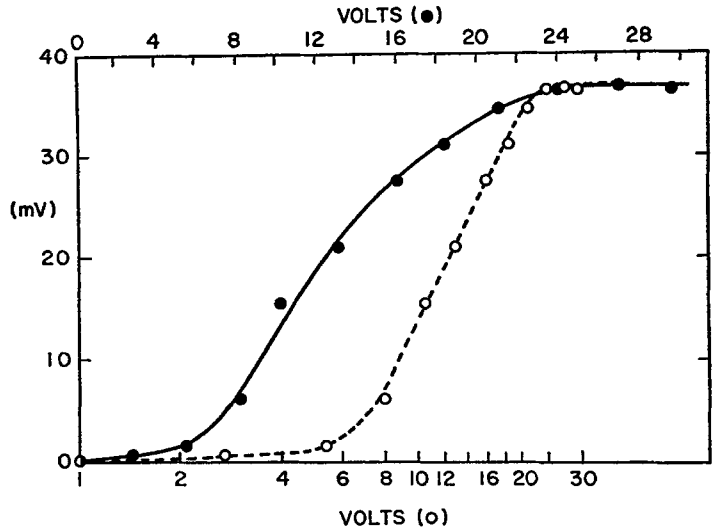

FIGURE 8. Linear (solid circles) and semilogarithmic (open circles) plots of generator potential as a function of displacement (the average of seven experiments). For seven points, a logarithmic relationship is clear. Threshold for individual cells varied from 2 to 6 mV, maximum stimulus from 18 to 30 mV.

cell. When a displacement causing a half maximal response was given at a frequency of up to 10/s, summation of the individual generator potentials (Fig. 11 A) was observed. With greater frequencies an initial summation was followed by a decrease of membrane potential (Fig. 11 B), which probably represents some adaptation of the hair cell's response. This adaptation lasted several seconds after high frequency stimulation.

Controls

To rule out movement artifacts, two types of control experiments were conducted. In the first type microelectrodes were inserted into photoreceptors (20–30 μm diameter) of the *Hermissenda* eye and optic ganglion cells (8–15 μm diameter). Displacements (sufficient for maximal stimulation of hair cells) of the eye and optic ganglion almost invariably caused no depolarization in the penetrated cell. Displacements 2–3 times those used to stimulate the hair cells maximally, rarely caused a photoreceptor or optic ganglion cell to depolarize before the electrode came out of the cell. When it did occur, this depolarization was small, not reproducible, and was followed by a gradual recovery of the resting membrane potential. Also, it was not graded with displacement magnitude.

A second type of control consisted of hair cell stimulation after the statocyst was drained of statolymph, by repeated microelectrode puncture of the cyst. The hair cells penetrated under these conditions showed typical spike size, membrane resistance, and spontaneous activity, but were not sensitive to

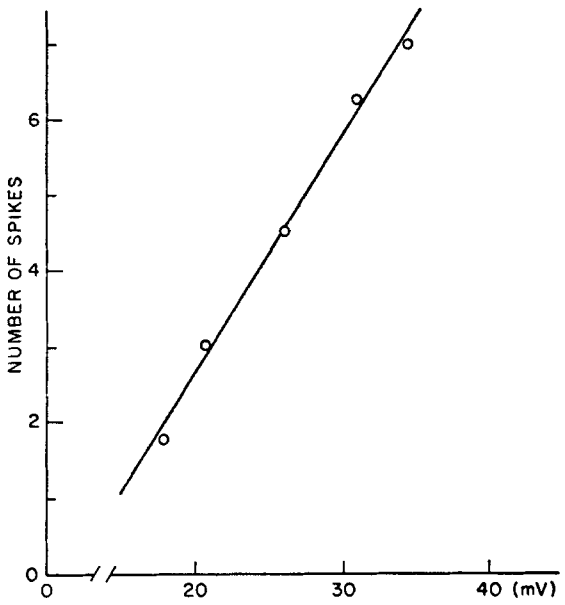

FIGURE 9 A. Spike frequency as a function of hair cell generator potential (average of four experiments). Spikes during first 60 ms of response to displacement were counted.

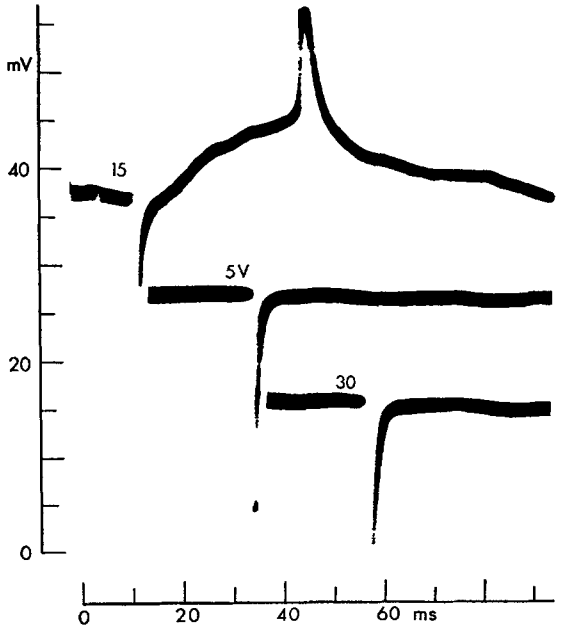

FIGURE 9 B. Hair cell response to displacement (15 V pulse) and recordings (lower two traces) when electrode is outside of the cell in the vicinity of the statocyst. The two lower records illustrate the stimulus artifact itself. The upper record demonstrates the resolution of latency possible within the technical limits of the experiment.

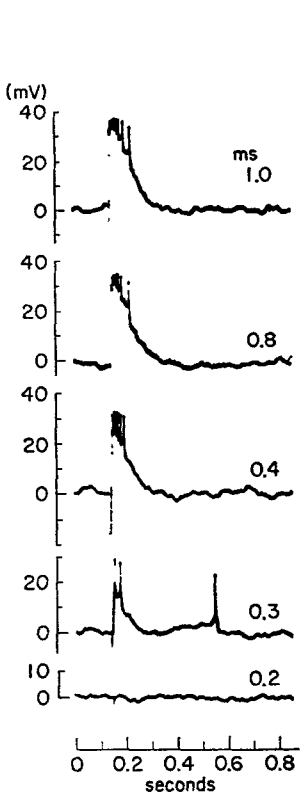

FIGURE 10

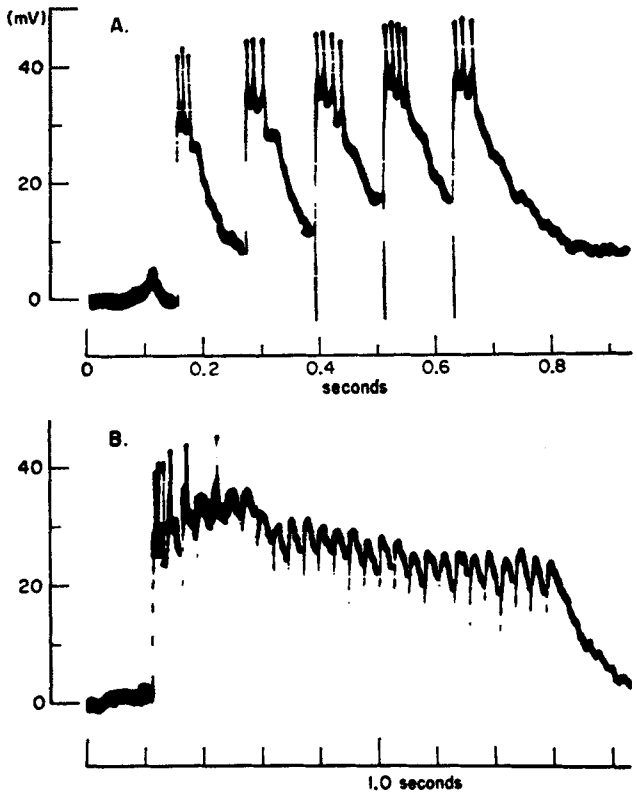

FIGURE 11

FIGURE 10. Hair cell responses for increasing duration of voltage pulses across the piezoelectric device. All pulses are 18 V. Duration increases from 0.2 to 1.0 ms. Maximum generator potentials begin with pulses of approximately 600 μs.

FIGURE 11. (A), Temporal summation of hair cell responses elicited by repeated displacements (1.0 ms duration) at a frequency of 10/s. Cell was slightly hyperpolarized to reduce spiking. (B), With higher frequency (20/s) responses initially summate and then progressively decrease.

displacements 2–3 times those sufficient to maximally stimulate the hair cells of an intact statocyst. (Very occasionally a hair cell of an intact cyst was insensitive to displacement. Such a cell was regarded as damaged and discarded.)

Conductance

As membrane potential was displaced from the resting level in the negative direction the magnitude of the generator potential increased (Fig. 12). As membrane potential was displaced in the positive direction the response decreased (Fig. 13). The plots of membrane potential and its sum with the generator potential vs. current injected (Fig. 14) form two lines until mem-

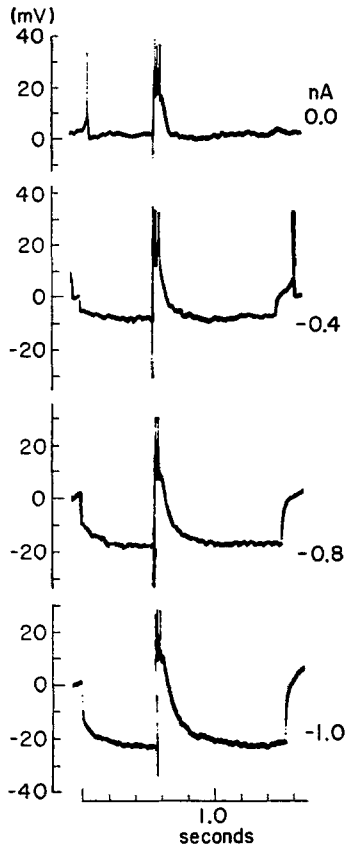

FIGURE 12

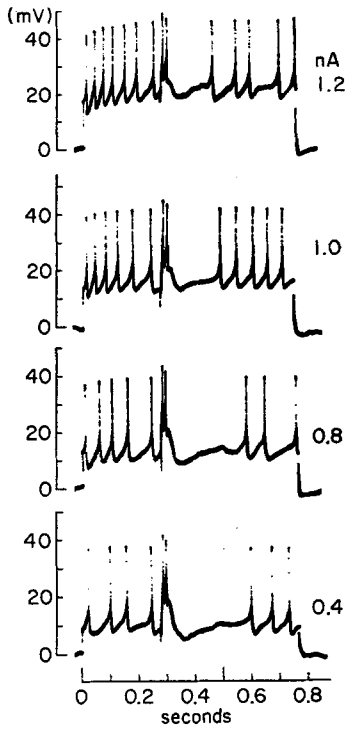

FIGURE 13

FIGURE 12. Effect of hyperpolarization on hair cell generator potential. A constant displacement is repeated as increasing hyperpolarizing current pulses are applied. Generator potential increases with more negative membrane potentials.

FIGURE 13. Effect of depolarization on hair cell generator potential. (For response at resting membrane potential, see Fig. 12.) A constant displacement (that used in Fig. 12) is repeated as increasing depolarizing current pulses are applied. Generator potential decreases with more positive membrane potentials. A hyperpolarizing wave follows the depolarizing generator potential for the first two current pulses. The generator potential is followed by an absence of spike activity for all levels of depolarization.

brane potential no longer increases linearly with increasing current injected (perhaps due to rectification of the membrane). The two lines appear tending toward intersection (before the nonlinearity of the potential-current relationship begins) and would intersect at a membrane potential of 30–35 mV. Thus, at a membrane potential between 30 and 35 mV the depolarizing generator potential would be abolished. These results are consistent with the generator potential arising from an increase in conductance to an ion whose equilibrium potential is between 30 and 35 mV.

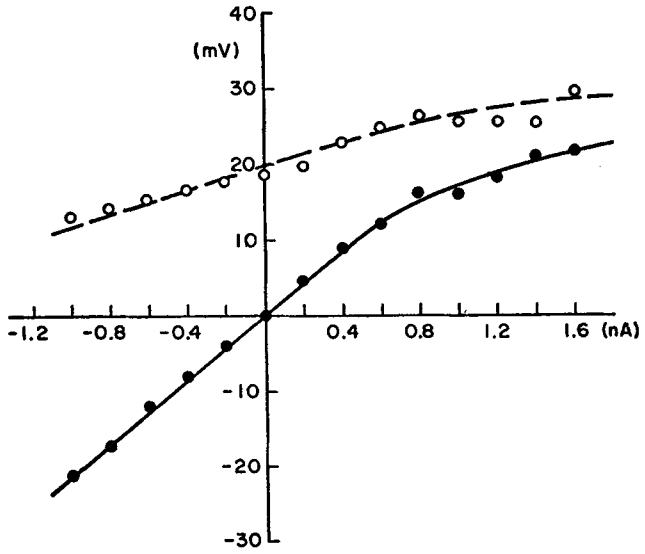

FIGURE 14. Current-voltage plots for hair cell membrane potential (solid circles) and generator potential (open circles). Plots are constructed from experiment of Figs. 12 and 13.

Hyperpolarizing Wave in Generator Potential

A small hyperpolarizing wave follows the depolarizing generator potential (Fig. 13) when the hair cell is depolarized, and the spikes produced by the depolarizing steps are blocked for 200–400 ms. This hyperpolarizing wave is seen in 10–15% of hair cells without prior depolarization of the membrane. Such cells usually achieve a maximal depolarizing generator potential less than 30 mV (Compared to 35–40 mV for other hair cells). Depolarization of these cells (Fig. 15) results in disappearance of the depolarizing generator potential and an increase in the hyperpolarizing wave. Hyperpolarization causes the depolarizing generator potential to increase in magnitude and also in duration, suggesting a reversal of the hyperpolarizing wave. This hyperpolarizing wave did not follow large depolarizing current pulses (causing a depolarization with superimposed spikes) of duration comparable to that of the generator potential. On one occasion a hair cell with no hyperpolarizing wave at resting potential was held for over 2 h. Toward the end of this period the cell began losing membrane potential, i.e., depolarized. Associated with this loss of membrane potential was the appearance of an increasingly more prominent hyperpolarizing wave after the depolarizing generator potential. These observations suggest then, that the slow hyperpolarizing wave may exist in all hair cell responses but is exaggerated by

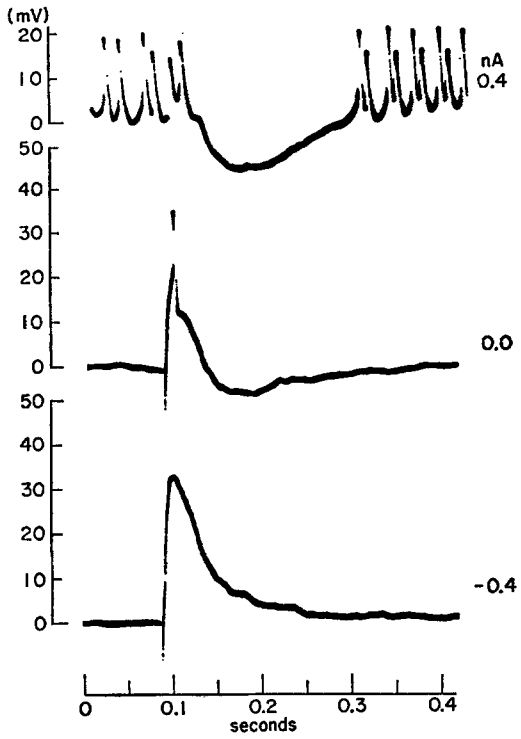

FIGURE 15. Effect of current on biphasic hair cell generator potential. Depolarization isolates a hyperpolarizing wave. Stimulus in upper trace occurs at break in the recording. Hyperpolarization broadens the depolarizing response and removes the hyperpolarizing wave suggesting its reversal.

depolarization resulting from positive currents or associated with the damage of penetration.

DISCUSSION

Hair cells in the statocyst of *Hermissenda crassicornis* respond to displacement with generator potentials up to 40 mV. Although hair cells in the *Necturus* lateral line are considerably larger, their responses are at least an order of magnitude smaller. This difference may either be a function of the recording techniques used or a real difference between responses of the two types of hair cells. Such a difference is not totally surprising if it is recalled that vertebrate hair cells do not have axons, and thus conducted action potentials, and perhaps large generator potentials, would not be necessary for information transmission to second order cells. By displacing membrane potential (Figs. 12, 13) it was shown that the hair cell generator potential might arise from a conductance increase. These results are similar to those obtained in the *Limulus* photoreceptor (Fuortes, 1959), the Pacinian corpuscle (Lowen-

stein and Ishiko, 1960) and in the crustacean stretch receptor (Terzuolo and Washizu, 1962). The generator potential in turn probably spreads to an excitable zone where spikes are triggered by membrane depolarization beyond a critical threshold. The sensory information is thus coded by the spikes whose frequency was shown to be directly proportional to membrane potential (Fig. 9). Such a spread of graded receptor potentials to a spike-generating focus is thought to occur in several kinds of receptors (Katz, 1950; Eyzaguirre and Kuffler, 1955; Fuortes, 1959; Thurm, 1965).

It was suggested (see Results) that damage might emphasize a hyperpolarizing wave observed in the displacement responses of 10–15% of hair cells. The initial depolarizing wave could arise from an increase in conductance of one ion and the later hyperpolarizing wave might arise from an increase in conductance of a second ion. This second conductance increase would always be present but might be more prominent in hair cells which had become depolarized by damage of microelectrode penetration. The later hyperpolarizing wave might arise, as does the depolarizing wave, from the hair cell's generator current, i.e., as a direct result of the displacement stimulus. Alternatively, the hyperpolarization might result from synaptic inhibition by other hair cells. Such inhibition does exist (Detwiler and Alkon, work in progress) and is presently under study.

Adequate Stimulation of Hair Cells

Light microscopic observation of the statoconia demonstrate that they collect in different regions of the statocyst for different spatial orientations of the isolated nervous system. Presumably the hair cell somata would move with the cyst, but the sensory hairs would be bent by the statoconia which move somewhat later. Such bending might also arise from a delay in the movement of the hair ends as they float in the statolymph. Stretching of membrane of the hair itself could be responsible for a conductance change and a resulting generator potential. Alternatively, bending could stretch membrane surrounding the apex of the hair where it inserts into the cell. Extracellular recordings (Wolff, 1970 *a*) indicated that molluscan hair cells respond to changes of the animal's position. Adequate stimulation of hair cells in the intact animal might arise, then, when the statoconia, affected by gravity, bend the sensory hairs. Although the statoconia would always be pulled by gravity in the same direction, different hair cells would be stimulated preferentially depending on the position of the animal.

It was shown that, for a certain range, the generator potential increases linearly with the logarithm of the displacement (Fig. 8). For any displacement, however, there must be acceleration of the cyst, the statoconia, and presumably of the hairs. Thus, a change in velocity, in addition to the actual movement, may affect the sensory hair. A rapid bending may be a more

effective stimulus than a slow bending of the hair just as rapid muscle stretching more effectively stimulates the muscle spindle (Ottoson and Sheperd, 1971). That displacement, independent of velocity, within the limits of the technique used in this study, effectively stimulates the hair cells is suggested by the experiment of Fig. 10. For a constant voltage, increasing duration of the stimulus increases the response until a plateau (0.6–1.0 ms) is reached. If the response only depended on velocity, decreasing responses would be expected as duration approached the time necessary for maximal excursion of the cyst (0.6 ms) when decreasing velocity must occur (Fig. 4). Since the hair cells may respond to displacement alone, independent of the rate of displacement, adequate stimulation could consist of bending the sensory hair irrespective of the bending velocity.

SUMMARY

(*a*) A technique is introduced using a piezoelectric device to stimulate hair cells of a molluscan statocyst while recording their responses intracellularly.

(*b*) Statocyst displacement produced with the technique was calibrated with stroboscopic photography.

(*c*) Properties of the hair cells' response to currents are studied. Two time constants are necessary to describe the hair cells' charging curves.

(*d*) For a certain range, the hair cell generator potential is shown to be a logarithmic function of displacement magnitude.

(*e*) Hair cell spike frequency is found to be a linear function of generator potential.

(*f*) Hair cell responses elicited by repeated displacements at a frequency of 10/s summate. With higher frequency the responses initially summate and then progressively decrease.

(*g*) The generator potential arises from a conductance increase to an ion with reversal potential of approximately 30–35 mV.

(*h*) A hyperpolarizing wave after the initial depolarizing generator potential is examined.

John Lewis was most helpful in much of the photographic processing used in this work. We are indebted to M. G. F. Fuortes, Peter Detwiler, and George Murray for their useful discussion of the material. Peter Detwiler was of great assistance in the preparation of histologic sections.

Received for publication 14 August 1972.

BIBLIOGRAPHY

COGGESHALL, R. E. 1969. A fine structural analysis of the statocyst in Aplysia californica. *J. Morphol.* **127**:113.

EYZAGUIRRE, C., and S. KUFFLER. 1955. Processes of excitation in the dendrites and in the soma of single isolated sensory nerve cells of the lobster and crayfish. *J. Gen. Physiol.* **39**:87.

FLOCK, A. 1965. Electron microscopic and electrophysiological studies on the lateral line canal organ. *Acta Oto-Laryngol. Suppl.* **199**:1.

FUORTES, M. G. F. 1959. Initiation of impulses in visual cells of Limulus. *J. Physiol. (Lond.).* **148**:14.

HARRIS, G. G., L. FISHKOPF, and A. FLOCK. 1970. Receptor potentials from hair cells of the lateral line. *Science* (*Wash. D. C.*). **167**:76.

JIELOT, R., A. SPOOR, and H. DEFRIES. 1952. The microphonic activity of the lateral line. *J. Physiol.* (*Lond.*). **116**:137.

KATZ, B. 1950. Depolarization of sensory terminals and the initiation of impulses in the muscle spindle. *J. Physiol.* (*Lond.*). **111**:261.

KUIPER, J. W. 1956. The microphonic effect of the lateral line organ. Publ. Biophys. Group, Natuurkundig laboratorium, Groningen. 1–159.

LOEWENSTEIN, W. R., and N. ISHIKO. 1960. Effects of polarization of the receptor membrane and the first ranvier node in a sense organ. *J. Gen. Physiol.* **43**:981.

OTTOSON, P., and G. M. SHEPERD. 1971. Transducer properties and integrative mechanisms in the frog's muscle spindle. *In* Handbook of Sensory Physiology. Springer-Verlag, Berlin. 1:442.

TERZUOLO, C. A., and Y. WASHIZU. 1962. Relation between stimulus strength, generator potential and impulse frequency in stretch receptor of crustacea. *J. Neurophysiol.* **25**:56.

THURM, U. 1965. An insect mechanoreceptor. Part II. Receptor Potentials. *Cold Spring Harbor Symp. Quant. Biol.* **28**:83.

TRINCKER, P. 1957. Bestandspotentiale im Bogengangssystem des Meerschweinchens und ihre Anderungen bei experimentellen Cupula-Ablenkungen. *Pflugers Arch. Gesamte Physiol. Menschen Tiere.* **264**:351.

VON BEKESY, G. 1960. Experiments in Hearing (Research articles from 1928 to 1958). McGraw Hill Book Company, New York.

WOLFF, H. G. 1968. Elektrische Antworten der Statonerven der Schnecken (Arion empiricorum und Helix pomatia) auf Drehreizung. *Experientia* (*Basel*). **24**:848.

WOLFF, H. G. 1969. Einige Ergebnisse zur Ultrastruktur der Statocysten von Limax maximus, Limax flavus und Arion empiriocorum (Pulmonata). *Z. Zellforsch. Mikrosk. Anat.* **100**:251.

WOLFF, H. G. 1970*a*. Statocystenfunktion bei einigen Landpulmonaten (Gastropoda). *Z. Vgl. Physiol.* **69**:326.

WOLFF, H. G. 1970*b*. Efferente Aktivitat in den Statonerven einiger Landpulmonaten (Gastropoda) *Z. Vgl. Physiol.* **70**:401.